Zeeman Effect

Jackson Lee, Taha Kaleem, David Petroski
Department of Physics, Rutgers University
(Dated: 11 October 2023)

The Zeeman splitting of several spectral lines of various atoms is tested and compared with theoretically obtained values and simulation. Gas discharge tubes for each element were placed in magnetic fields of varying strength. For each emission line, a range of frequencies around the original spectral line were tested, and the photon count at each frequency recorded. The spectra in the presence of the magnetic field were found to be consistent with theoretical predictions.

Introduction and Theory

Photon emission from an atom occurs when the atom returns from an excited state to a ground state. As electrons in atoms are characterized by a set of discrete energy states, the emitted photons are observed to have a discrete spectrum. When the spectrum is observed with a spectrometer, however, the emission lines have some width due to the finite resolution of the spectrometer.

In the Zeeman effect, the energy levels shift in the presence of a magnetic field. Specifically, without a magnetic field, there is a degeneracy in the energy levels of the atom, as for each level defined by an orbital quantum number l and a principal quantum number, there are $2l + 1$ possible states with different projections of angular momentum along a given axis. In the presence of a magnetic field along that axis, the energy shift of that level is dependent on the angular momentum along that axis, thus breaking the degeneracy. As shown in figure 1, this leads to splitting of spectral lines.

In reality, the spin angular momentum s must also be considered. In this case, the total angular momentum j can take any value between l-s and l+s, and the momentum m_j along an axis can take on values between -j and j. In this case, we calculate the Lande g-factor of a state as:

$$g_L = 1 + \frac{J(J+1) + S(S+1) - L(L+1)}{2J(J+1)}$$

And the effective g-value of a transition is:

$$g_{eff} = g_L m_j - g'_L m'_j$$

With the primed values corresponding to the upper level. The shift in the emitted wavelength can then be calculated as:

$$|\Delta\lambda| = \frac{g_{eff}\lambda^2\mu_B B}{hc} = 4.668 \times 10^{-8} g_{eff}\lambda^2 B$$

Where μ_B is the Bohr Magneton.

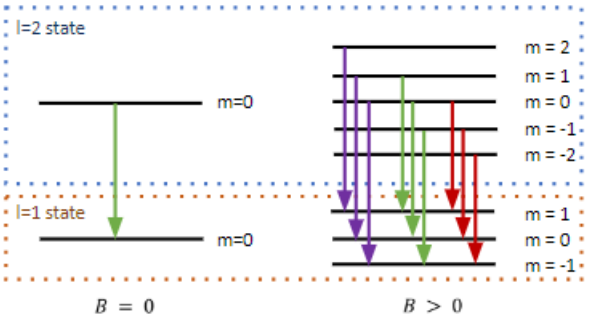

Figure 1: Zeeman effect in l = 2 and l = 1 states. Under no magnetic field (left), we have one spectral line, and under a magnetic field (right), we have more states associated with $m = -l, l + 1, \ldots l$, and we will see two more spectral lines compared to the zero magnetic field case.

The Zeeman effect is further complicated by differences in polarization for different emissions: emissions where the m_j value changes are polarized perpendicular to the magnetic field, and are called sigma lines, while lines where the m_j value remains constant are called pi lines.

In this lab, we test the above equation by testing the Zeeman splitting for various spectral lines in various materials and varying the magnetic field. We expect the relation between the splitting and the magnetic field to be linear and calculate the g_{eff} from the observed relation between splitting and magnetic field.

Apparatus and Procedure

To stimulate photon emission from the gas discharge tubes, we apply a 5000V electric current across the tube. We use a large electromagnet to vary the magnetic field in a certain region of the discharge tube. We adjust the strength of the magnetic field by adjusting the current fed into the electromagnet.

To observe the emitted spectrum, we place an optical device with an adjustable polarizer lens next to the discharge tube, allowing us to observe the region in the magnetic field. From there, a fiber optic cable then transmits the light into a spectrometer. The photon counts are then recorded by a computer connected to the spectrometer.

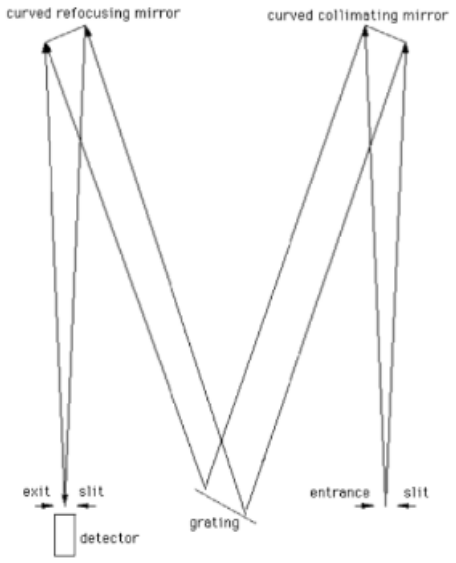

Figure 2: Czerny-Turner Scanning Spectrometer

The spectrometer used in this experiment was a Czerny-Turner Scanning Spectrometer. As seen in Figure 2, the spectrometer emits light through an entrance slit of controllable width, where it then is reflected to a curved collimating mirror and diffracted by a grating, before being refocused by another mirror. The light is then reflected off a mirror and diverted toward a photomultiplier photon detector.

The electromagnet used to apply the magnetic field to the gas tube consisted of a ring-shaped ferromagnetic core, with a short gap in which the tube sits. Coils of wire were wrapped around the core to magnetize it. By varying the current passed through the wires, we controlled the magnetic field in the gap.

To measure the strength of the magnetic tube, we utilized a small Hall probe inserted into the gap, which consisted of a small magnetic field sensing circuit on the end of a thin, flat board. By utilizing the Hall effect, the output voltage of the sensor is directly proportional to the field strength. The integrated circuit was then connected to a digit meter, from where we could ascertain the magnetic field.

Magnetic hysteresis is important to account for in this lab, as ferromagnetic materials retain some magnetization when an applied field is removed. We establish a magnetic hysteresis curve, as whenever we change the applied magnetic field, we retain some magnetization. This in turn alters the way in which the ferromagnet responds to another field. As a result, the field strength produced by the ferromagnet is dependent not only on the magnetizing force, but also on the initial magnetization. To correct for this, we degaussed the electromagnet (brought magnetization to 0) to ensure that the initial conditions were as similar as possible, and that the magnetic field could be well adjusted by the applied current. Degaussing consisted of varying the current from 10 amps to -9 amps, to 8 amps, and so on until we reached 0 amps. We show the Hysteresis curve for the up branch in figure 3, taken for two different days.

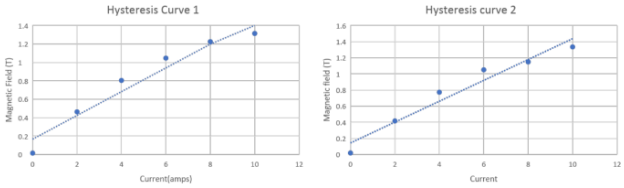

Figure 3: Hysteresis curve for the up branch, taken for 2 different days. The magnetic field is measured in the gap in the electromagnet.

For data collection, we place the discharge tube of the chosen material in the electromagnet and connect high voltage contacts to the electrodes on either side. We first measure the spectra with zero current passing through the electromagnet, meaning that the magnetic field is near zero in the region being observed. To ensure that the field is indeed zero, we take magnetic field strength measurement in this location. We then set the polarizer to 114 degrees to observe the pi polarized spectrum, and 24 degrees for the sigma polarized spectrum. We program the spectrum analyzer to record the number of photons

found in 0.0005/0.001 nm intervals over a 0.5 second interval. We repeat the process for field strengths corresponding to 10, 8, 6, 4, and 2 amperes of current, for several different emission lines, and for the sigma polarized spectra each time.

Data and Analysis

For Mercury, we measure the spectra of the $^3S_1$ to $^3P_0$, $^3S_1$ to $^3P_1$, and $^3S_1$ to $^3P_2$ transitions respectively. For Neon, we measure the $^3S_1$ to $^1P_1$ transition. We first present theoretical predictions of the Zeeman splitting for these spectral lines. Using the results in the introduction and theory, we compute theoretical values of g_{eff} for the three Mercury lines. These results are shown in table 1.

Wavelength (nm)	m'_j	m_j	Polarization	g_{eff}
404.7	1	0	Sigma	-2
404.7	0	0	Pi	0
404.7	-1	0	Sigma	2
435.8	1	1	Pi	-1/2
435.8	0	1	Sigma	3/2
435.8	1	0	Sigma	-2
435.8	0	0	Pi	0
435.8	-1	0	Sigma	2
435.8	0	-1	Sigma	-3/2
435.8	-1	-1	Pi	1/2
546.1	1	2	Sigma	1
546.1	1	1	Pi	-1/2
546.1	1	0	Sigma	-2
546.1	0	1	Sigma	3/2
546.1	0	0	Pi	0
546.1	0	-1	Sigma	-3/2
546.1	-1	0	Sigma	2
546.1	-1	-1	Pi	½
546.1	-1	-2	Sigma	-1

Table 1: G_{eff} for all allowed transitions for 3 Mercury lines, along with the corresponding polarization of the emitted photon.

We then analyze the effect of both Doppler broadening and instrumental resolution on the spectral line width. The Doppler broadening for the 546.1 nm Mercury line is calculated as:

$$\Delta\lambda = 2\lambda_0\sqrt{\frac{2ln2kT}{m_0c^2}} = 0.0006\,nm$$

By comparison, the resolution of the spectrometer is 0.006 nm. As the 546.1 nm line will have the greatest Doppler broadening, we can be confident that the Doppler broadening is lower than the instrumental resolution. Therefore, the resolution of the spectrometer is the determining factor in the resolution of the spectral lines. To resolve observed spectral lines, we need the Zeeman splitting to be greater than the instrumental resolution, or:

$$4.668 \times 10^{-8}\Delta g_{eff}\lambda^2 B > \Delta\lambda_{instrumental}$$

to resolve transitions with different effective g values.

For the $^3S_1$ to $^3P_0$ transition, the sigma lines exist at effective g values of 2 and -2, and so a B field of **0.196** Teslas is required to resolve the peaks. In comparison, for the $^3S_1$ to $^3P_1$ transition, the closest sigma lines exist at effective g values of 3/2 and 2, and therefore a B field of **1.35 Teslas** would be required to resolve the closest sigma lines. Similarly, the closest pi lines exist at effective g values of 0 and ½, and again a B field of **1.35 Teslas** would be required to resolve the pi lines.

In our experiment, the magnetic field is not strong enough to resolve these sigma and pi lines. In accounting for instrumental resolution, then, we expect that the sigma lines at g_{eff} = 1, 3/2, 2 will appear as a single peak, and similarly for the pi lines. We can then calculate the g_{eff} that we expect to observe, by taking the weighted average of these g_{eff} values, weighted by the transition intensities shown in figure 4. The results are shown in table 2.

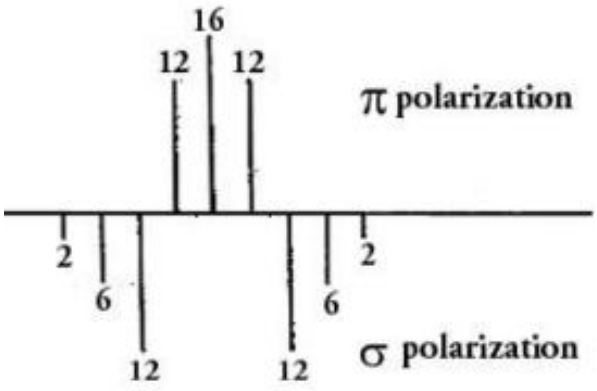

Figure 4: Transition intensities for pi polarized and sigma polarized transitions, corresponding to g_{eff} = -0.5, 0, 0.5 for pi transitions, and g_{eff} = 1, 3/2, 2 for sigma transitions, with corresponding negative values.

Material	Zeeman effect Transition	Normal photon wavelength (nm)	Expected g_{eff}
Mercury (Hg)	$^3S_1$ to $^3P_1$	435.8	2
Mercury (Hg)	$^3S_1$ to $^3P_2$	546.1	1.625
Mercury (Hg)	$^3S_1$ to $^3P_0$	404.7	1.25
Neon (Ne)	$^1S_0$ to $^1P_1$	585.3	1

Table 2: Expected sigma g_{eff} for 3 Mercury lines and 1 Neon line, taking instrumental resolution into account.

We then conduct our experimental procedure to obtain real spectra. The detected photon counts are shown as scatter plots for select emission lines and magnetic field strengths in figures 5 and 6.

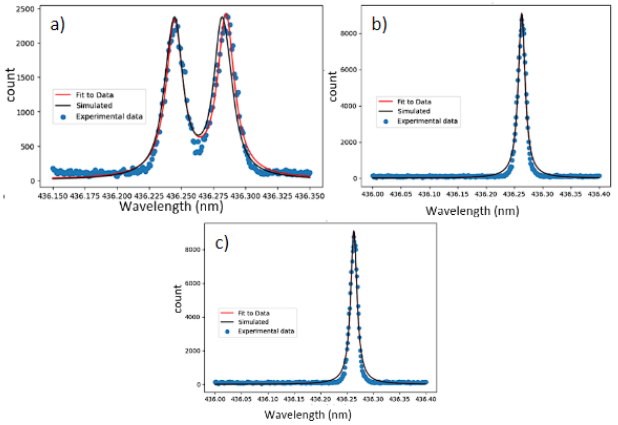

Figure 5: Observation of Zeeman effect of $^3S_1$ to $^3P_1$ transition in Mercury (435.8 nm). Plots show Photon count versus observed wavelength from experimental spectroscopy results with a Lorentzian fit and simulation-based calculations. a) Observed splitting of sigma lines (~.04 nm) at 1.334 T. b) Observed pi line at 1.334 T. c) Observed pi line at no applied magnetic field (ambient field of 0.019 T)

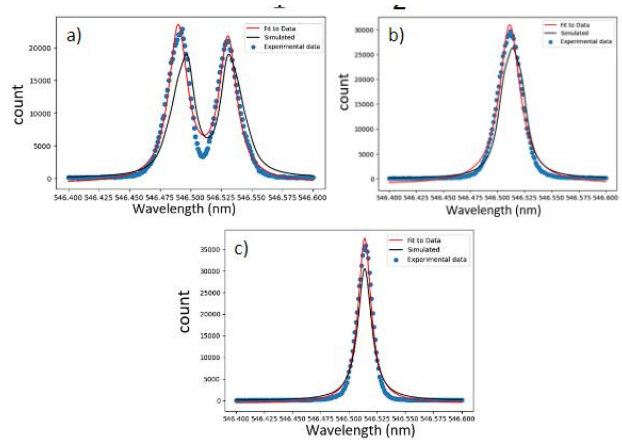

Figure 6: Observation of Zeeman effect of 3S1 to 3P2 transition in Mercury (546.1 nm). Plots show Photon count versus observed wavelength from experimental spectroscopy results with a Lorentzian fit and simulation-based calculations. a) Observed splitting of sigma lines (~.04 nm) at 1.17 T. b) Observed pi line at 1.17 T. c) Observed pi line at no applied magnetic field (ambient field of 0.015 T)

The full dataset of observed spectra is shown in the appendix. We note that the peak positions are consistently ~0.4 nm offset from the theoretical peak positions, which we attribute to an inherent offset in the spectrometer. As this offset affects all peaks equally, we do not expect that this will change the observed peak splittings.

We see from the figures that peak splittings are indeed observed in the presence of a magnetic field, for sigma polarized spectra. For pi polarized spectra, we see a broadening of the line width in the presence of a magnetic field.

As seen in figures 3, 4, and in the appendix, we fit a Lorentzian curve(s) to the data, allowing us to easily ascertain the peak wavelengths of the spectra. Having fit Lorentzian curves to the data, we plotted the peak splittings for different sigma polarized spectral lines against the applied magnetic field. The results for the 4 spectral lines are shown in Figure 7.

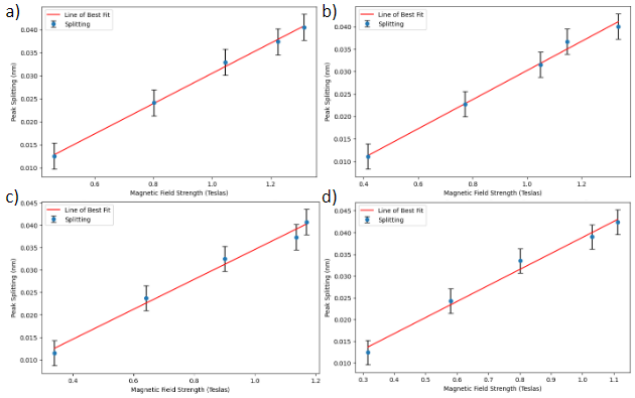

Figure 7: Observed sigma line splittings versus magnetic field strength with line of best fit. a) Observed splittings for Hg 404.7 nm lines, ie 3S1 to 3P0 transition b) Observed splittings for Hg 435.8 lines, ie 3S1 to 3P1 transition c) Observed splittings for Hg 546.1 lines, ie 3S1 to 3P2 transition. d) Observed splittings for Neon 585.3 lines, ie 1S0 to 1P1 transition.

As seen in Figure 7, the observed splitting is linear with respect to the applied magnetic field, which is what we expect from theory. For each observed splitting, we empirically assign a peak position error of +/- 0.002 nm, and use propagation of

errors to find the error in the peak splitting. These error bars are shown in Figure 7.

For each spectral line, we make a line of best fit between the applied magnetic field and the observed splitting. As shown in the introduction and theory, this gives us a ratio between the magnetic field and observe splitting, allowing us to easily calculate the g_{eff} for each spectral line, with corresponding error. We show these results in Table 3.

Material	Zeeman effect Transition	Normal photon wavelength (nm)	g_{eff} value
Mercury (Hg)	$^3S_1$ to $^3P_1$	435.8	1.8 +/- 0.2
Mercury (Hg)	$^3S_1$ to $^3P_2$	546.1	1.2 +/- 0.1
Mercury (Hg)	$^3S_1$ to $^3P_0$	404.7	2.1 +/- 0.3
Neon (Ne)	$^1S_0$ to $^1P_1$	585.3	1.2 +/- 0.1

Table 3: G_{eff} calculated from lines of best fit between magnetic field and Zeeman splitting for 4 spectral lines.

We see that the theoretically expected g_{eff} values, when accounting for instrumental resolution, match the observed values from table 1 within error bars for all Mercury lines. For Neon, there is a small discrepancy, which we attribute to approximation error in the Russell-Saunders coupling. However, for Neon, we still see that the observed g_{eff} closely matches theory, and that the g factor of the initial state is indeed 0, and the g factor of the final state is 1.

To further confirm the fit of our experimental data to the theoretical expectation, we ran simulations for the Mercury $^3S_1$ to $^3P_1$ and $^3S_1$ to $^3P_2$ transitions. Using the g_{eff} values from table 1, we find the expected peak positions at different magnetic fields. We then take the peaks to be Lorentzians with full width at half maximum determined by the instrumental resolution and peak amplitude determined by the transition intensities in Figure 4, and take the sum of the Lorentzians to be the simulated result. The simulated results, normalized to match the total photon count of the experimental results, are shown in figures 5, 6 and appendix. We see that the simulated results match our experimental data well, further bolstering the strength behind the Zeeman effect's theory.

By using the theoretically predicted values of g_{eff}, we can also calculate the electron charge to mass ratio, using $\mu_B = e\hbar/(2m_e)$, and again using the observed splitting to magnetic field ratio. Doing so for the Mercury $^3S_1$ to $^3P_0$ line, we find a charge to mass ratio of **1.8 +/- 0.2 x 10^{11} C/kg.** Repeating the procedure for the $^3S_1$ to $^3P_1$ transition, we find that a charge to mass ratio of **2.0 +/- 0.2 x 10^{11} C/kg.** The first value agrees with the theoretical value of 1.76×10^{11} C/kg within error bars, while the second value barely disagrees. We hypothesize that error in the measurement of the magnetic field due to the sensitivity of the Hall probe to orientation, as well as noise in the spectrum, may have contributed to this result.

Conclusion

We obtain spectra for several different emission lines in Mercury and Neon, subject to varying magnetic field strengths, allowing observation of the Zeeman effect. We clearly see splitting of the spectral lines, as well as a linear relation between the splitting distance and the external magnetic field. We calculate effective g values for each spectral line, as well as electron charge to mass ratio. We find that the effective g values match theoretical predictions within error bars when accounting for limitations in instrumental resolution for Mercury, while closely matching predictions for the observed Neon line. We also find that theoretical simulations fit our experimental data well. We further find that the electron charge to mass ratio matches the accepted value well, with only very small discrepancies. Our results indicate that the Zeeman effect can indeed be experimentally observed and verified, and matches quantum mechanical theory well.

References

1. Lab Manual, The Zeeman Effect, Department of Physics and Astronomy, Rutgers University.

Appendix

Here, we show the raw data obtained, in the form of graphs of the spectra. Spectra are fitted with single peaked or double peaked Lorentzians.

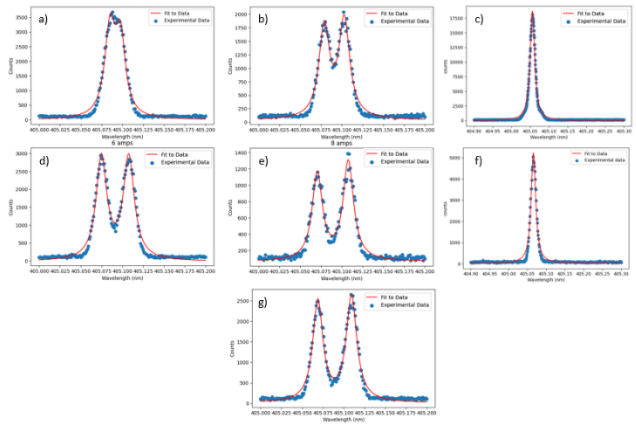

Figure A1: Zeeman shift of Hg 404.7 nm lines, ie 3S1 to 3P0 transition, given by Phonon count versus wavelength (Experimental results with Lorentzian fit). a) Sigma line splitting at 0.463 T. b) Sigma line splitting given by 0.803 T. c) Pi line splitting given by 1.313 T. d) Sigma line splitting given by 1.045 T. e) Sigma line splitting given by 1.224 T. f) Pi line splitting given by 0.015 (no applied current in magnet) T. g) Sigma line splitting given by 1.334 T.

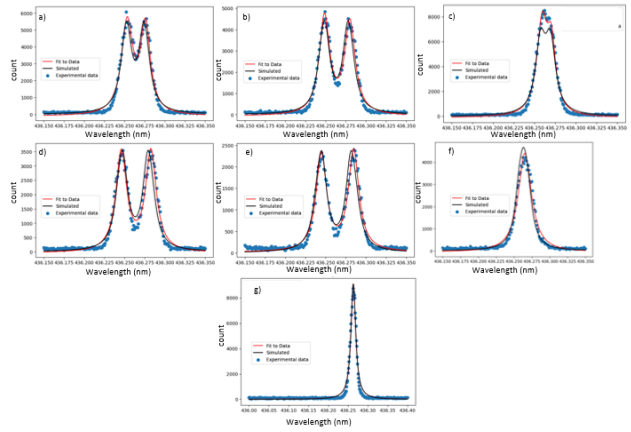

Figure A2: Zeeman splitting of Hg 435.8 nm lines, ie 3S1 to 3P1 transition, given by Phonon count versus wavelength (plotted simulation, and experimental results with Lorentzian fit). a) sigma line splitting observed at 0.772 T. b) Sigma line splitting observed at 1.05 T. c) Sigma line splitting observed at 0.419 T. d) Sigma line splitting observed at 1.148 T. e) Sigma line splitting observed at 1.334 T. f) Pi line observed at 1.334 T. g) Pi line observed at 0.019 T (no applied current in magnet).

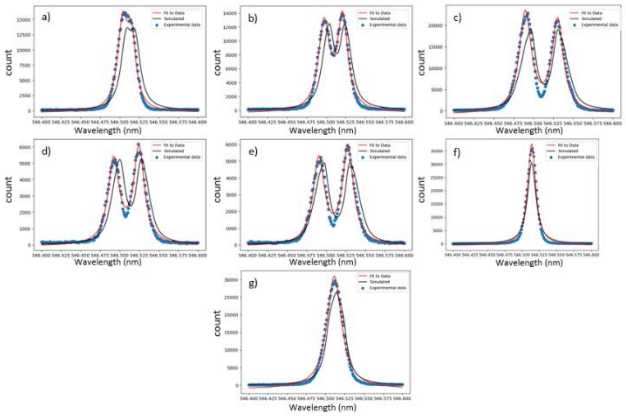

Figure A3: Zeeman splitting of Hg 546.1 nm lines, ie 3S1 to 3P2 transition, given by Phonon count versus wavelength (plotted simulation, and experimental results with Lorentzian fit). a) sigma line splitting observed at 0.34 T. b) Sigma line splitting observed at 0.642 T. c) Sigma line splitting observed at 1.17 T. d) Sigma line splitting observed at 0.901 T. e) Sigma line splitting observed at 1.136 T. f) Pi line observed at 0.015 T (no applied current in magnet). g) Pi line observed at 1.17 T.

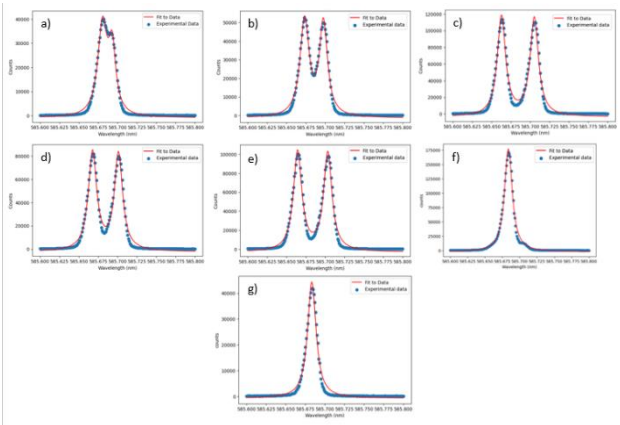

Figure A4: Zeeman splitting of Neon 585.3 lines, ie 1S0 to 1P1 transition, given by Phonon count versus wavelength (Experimental results with Lorentzian fit). a) sigma line splitting observed at 0.316 T. b) Sigma line splitting observed at 0.58 T. c) Sigma line splitting observed at 1.112 T. d) Sigma line splitting observed at 0.802 T. e) Sigma line splitting observed at 1.03 T. f) Pi line observed at 1.112 T (no applied current in magnet). g) Pi line observed at 0.0933 T (no external current applied to magnet).